JOURNAL OF MODERN OPTICS
2003, VOL. 50, NO. 15–17, 2523–2542

Taylor & Francis
Taylor & Francis Group

Whispering gallery mode based optoelectronic microwave oscillator

A. B. MATSKO, L. MALEKI, A. A. SAVCHENKOV and V. S. ILCHENKO

Jet Propulsion Laboratory, California Institute of Technology, 4800 Oak Grove Drive, Pasadena, CA 91109-8099, USA

(*Received 2 March 2003*)

Abstract. Properties of the optoelectronic microwave oscillator (OEO) based on an optical whispering gallery mode lithium niobate disc cavity are studied theoretically. We show that the threshold of the oscillation of this device may be as low as 1 mW, and its frequency stability (Allan deviation) may be as small as $10^{-15}/t^{1/2}$ for reasonable experimental conditions. The properties of resonant and non-resonant OEOs are compared. Preliminary experimental results on the whispering gallery mode OEO are reported.

1. Introduction

Generation of spectrally pure signals at 1 to 100 GHz supports new developments in communications, radar and navigation. The advent of high throughput optical communications links points to the prospects for networks operating at data rates as high as 160 Gbs^{-1} and consisting of multiples of channels separated by a few gigaHertz. Schemes for realizing this type of capability rely on sources able of providing high frequency, low phase noise signals, without which an efficient high data rate system would not be possible. Similarly, high performance radar systems require low phase noise oscillators to allow detection of feeble signals from the dense background clutter.

The optoelectronic oscillator (OEO) is a device that produces spectrally pure signals at many tens of gigaHertz based on photonic techniques, and thus overcomes some of the inherent limitations of the conventional electronic devices [1–7]. The OEO is a generic architecture consisting of a laser as the source of light energy. The laser radiation propagates through a modulator and an optical energy storage element, before it is converted to electrical energy with a photodetector. The electrical signal at the output of the modulator is amplified and filtered before it is fed back to the modulator, thereby completing a feedback loop with gain, which generates sustained oscillation at a frequency determined by the filter.

Since the noise performance of an oscillator is determined by the energy storage time, or quality factor Q, then the use of optical storage elements allows for the realization of extremely high Q's and thus spectrally pure signals. In particular, a long fibre delay allows realization of micro-second storage times, corresponding to Q's of about a million at 10 GHz oscillation frequency. This is a high value compared to conventional dielectric microwave cavities used in oscillators [8, 9]. The fibre delay line also provides for wide-band frequency

Journal of Modern Optics ISSN 0950–0340 print/ISSN 1362–3044 online
http://www.tandf.co.uk/journals
DOI: 10.1080/0950034032000121037

operation unhindered by the usual degradation of the oscillator Q with increasing frequency. Thus, spectrally pure signals at frequencies as high as 43 GHz, limited only by the modulator and detector bandwidth, have been demonstrated.

These and other salient features of the OEO have been previously analysed and several variations based on multi-loop operations have been considered. In particular, a version that places a light source within the optoelectronic feedback loop, which generates simultaneously spectrally pure microwaves and short optical pulses, was suggested and realized. This configuration, dubbed as the coupled optoelectronic oscillator (COEO) is similar to actively mode locked lasers, with the major distinction that a COEO contains its own high performance microwave drive source [10–12].

The OEO is similar to a microwave oscillator in all but one key feature. In a microwave oscillator, stability is achieved through the stored microwave energy in a high-Q microwave resonator, and the oscillation frequency is locked to the frequency of the resonator. In an OEO the microwave energy, being carried as modulated light phase and/or amplitude, is stored in an optical delay line or an optical resonator. Thus, with the OEO there is no need for a microwave cavity. A long optical fibre at room temperature, for example, does the same function as a high-Q microwave resonator does at the liquid-nitrogen temperature.

The process of imprinting the microwave field on the light carrier is achieved by an electro-optical modulator (EOM). The transformation of the modulated light power into a microwave signal is obtained via a photodetector. Hence, in an OEO the laser light energy is converted directly to spectrally pure microwave signals, using an electro-optic feedback loop containing a high-Q optical element, at a frequency limited only by the available optical modulation and detection elements.

The EOM is one of the main sources of power consumption in the OEO because of the large power required to drive the conventional modulators. Both broadband Mach–Zehnder modulators and free space microwave cavity-assisted narrow-band modulators typically require one to a few watts of microwave power to achieve a significant modulation. This means that either the photocurrent in the OEO system should be amplified significantly, or a powerful laser should be used as the source of the drive power for the OEO. If the microwave power is small, the information about the microwave signal simply will not be transduced to light through the EOM.

By utilizing a high-Q resonance, instead of the zero-order interferometry, as the basis for electro-optic modulation one can reduce the controlling power by many orders of magnitude and reduce the energy consumption of the OEO. For this purpose, the dielectric cavities with whispering gallery modes (WGMs) are useful. Because of their extremely high-Q and small mode volumes, the field density in the WGMs of these optical cavities is extremely high. This feature was put to advantage in realizing high efficiency active elements, such as lasers with doped glass [13–15], and modulators based on the electro-optic effect [16–18]. The latter devices are important elements that can be combined with some of the unique features of the OEO to realize the configuration needed for many of the applications mentioned above.

In this paper we study the properties of the optoelectronic oscillator based on whispering-gallery mode electro-optical modulators. We compare the properties of these novel devices with the characteristics of a conventional OEO which includes

a non-resonant planar EOM. We show that the low threshold and low power consumption are the advantages of the resonant OEO compared with the non-resonant one. The disadvantages are low saturation and low output power, and a possibility of transforming the noise of the light field into the microwave signal. In general, resonant and conventional OEOs have non-overlapping characteristics and are both useful depending on the application.

The paper is organized as follows. In section 2 we discuss the value of threshold power, oscillation frequency and phase diffusion for resonant OEO based on WGM EOM. In section 3 we recall properties of conventional OEO. Similarities and differences of the devices are discussed in section 4. Finally, in section 5, we present data of a proof-of-principle experiment with an OEO based on an integrated WGM cavity modulator.

2. Resonant optoelectronic oscillator

In this section we describe properties of a resonant OEO based on a whispering gallery mode electro-optic modulator. We derive expressions for the oscillation threshold, and determine the oscillation frequency and noise properties of the device.

2.1. *Set-up and basic equations*

The optoelectronic oscillator based on the whispering gallery mode is depicted in figure 1. Monochromatic light from a laser is launched into a Mach–Zehnder interferometer formed by a fibre delay line in one arm and a toroidal lithium niobate cavity in the other. The light from one output port of the interferometer is used as a signal, while light from the other output port is sent into a feedback loop formed by a delay line, photodiode, filter, amplifier and the microwave resonator.

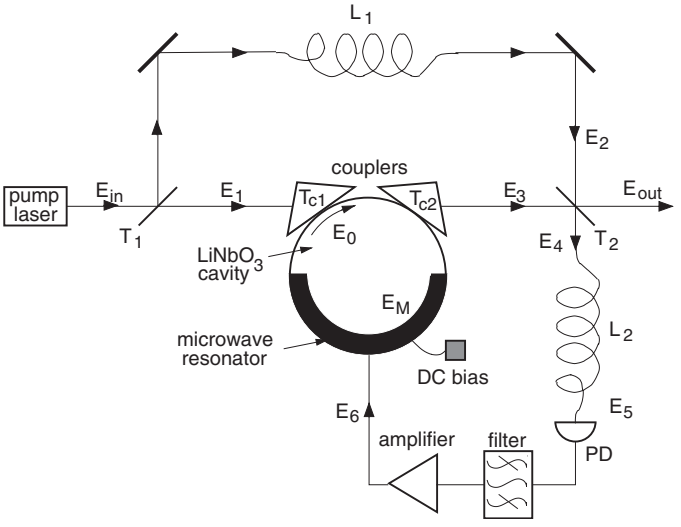

Figure 1. Opto-electronic oscillator based on whispering gallery mode $LiNbO_3$ cavity integrated with a microstrip microwave resonator.

The filter and the amplifier may be eliminated under certain conditions, discussed below.

Let us write the expressions that describe the operation of this system. The electric field after the first beam splitter (see in figure 1) is

$$E_1(t) = E_{\rm in}(t)T_1^{1/2} - \hat{e}_{\rm d1}(t)(1 - T_1)^{1/2}, \tag{1}$$

where $E_{\rm in}(t)$ is the input field, T_1 is the energy transmission coefficient of the input beamsplitter and $\hat{e}_{\rm d1}$ is the dark port quantum noise. We assume that the response of the beam splitter does not produce a delay. Here and below we consider the optical energy as a running wave, i.e. the complex field amplitude E may be presented as $|E|^2 = 2\pi P/(\mathcal{A}cn)$, where P is the light power in vacuum, $\mathcal{A}$ is the cross-sectional area of the fibre and n is the refractive index of the material. The total, time averaged, energy stored in a fibre with length L is, therefore, $n^2(2|E|^2)\mathcal{A}L/(4\pi) = PLn/c = P\tau$, where τ is the propagation time of light in the fibre.

Light, characterized by electric field E_1, is subsequently sent into a resonant electro-optic modulator based on the lithium-niobate toroidal cavity coupled to a microstrip microwave resonator, described in detail in [18]. The cavity may be fabricated from commercial flat Z-cut $LiNbO_3$ substrate. It is a disc with radius a and thickness $d \ll a$. The rim of the disc is polished such that the cavity becomes a part of an oblate spheroid. The extraordinary axis of $LiNbO_3$ coincides with the symmetry axis of the cavity.

Light is launched into, and retrieved from, the optical cavity via a pair of coupling prisms. The index of refraction of the prisms must exceed the index of refraction of the cavity whispering gallery modes n_0, in order to create an efficient coupling. The entrance and exit coupling prisms may be characterized by the energy transmission coefficients $T_{\rm c1}$ and $T_{\rm c2}$, respectively.

The electric field of light, E_0, which circulates inside the cavity, may be expressed as

$$E_0(t) = E_1(t)T_{\rm c1}^{1/2} + \hat{e}_{\rm d2}(t)T_{\rm c2}^{1/2} + E_0(t - \tau_{\rm c} - \tau_{\rm B} - \tau_{\rm M}(t))(1 - T_{\rm c1} - T_{\rm c2})^{1/2}, \tag{2}$$

where $\hat{e}_{\rm d2}$ is the dark port quantum noise of the second coupler, $\tau_{\rm c} = 2\pi a n_0/c$ is the cavity round trip time, $\tau_{\rm B}$ is a DC bias time shift and $\tau_{\rm M}(t)$ is the delay time that results from the interaction of the microwave field with light

$$\tau_{\rm M}(t) = \frac{n_0^2}{2^{1/2}} r_{\rm eff} \int_0^{\tau_{\rm c}/2} (E_{\rm M}(t + t') + E_{\rm M}^*(t + t')) \cos\left(\frac{2\pi t'}{\tau_{\rm c}}\right) {\rm d}t'. \tag{3}$$

Here n_0 is the refractive index of $LiNbO_3$ at light frequency, $r_{\rm eff}$ is the effective electro-optic constant for $LiNbO_3$ [19], and $E_{\rm M}(t)$ is the complex microwave field amplitude averaged over the mode volume. Expression (3) was derived using the following assumptions. (i) The electric field in the microwave resonator depends on its location. It has maxima at the ends of the resonator and zero at the centre of the resonator. We approximate this dependence by a cosine function. (ii) The microwave resonator covers a half of the optical cavity along its rim. (iii) The microwave field smoothly overlaps the volume where light propagates. The half-wave microstrip resonator may be fabricated by placing a half-circular electrode along the rim of the optical $LiNbO_3$ cavity. By tuning the length of the stripline

electrodes the resonator can be tuned to a frequency equal the optical free spectral range of the microresonator.

Light propagating along the rim of the optical cavity encounters the microwave field amplitude in accordance with the expression $2^{1/2}(E_{\mathrm{M}}(t+t')+E_{\mathrm{M}}^{*}(t+t'))\cos(2\pi t'/\tau_{\mathrm{c}})$, where time t' describes light propagation and $t'=0$ is chosen to be the relative moment of time when light enters into the resonator. The factor $2^{1/2}$ results from our assumption that $E_{\mathrm{M}}(t)$ is the average complex field amplitude, while at the ends of the resonator the absolute value of the amplitude is $2^{1/2}$ times larger. The moment of time when light exits the resonator is, therefore, $t'=\tau_{\mathrm{c}}/2$. The resulting delay of the light wave is obtained via integration over the interaction time.

To simplify equation (3) we assume that $E_{\mathrm{M}}(t)=\widetilde{E}_{\mathrm{M}}(t)\exp(-\mathrm{i}\omega_{\mathrm{M}}t)$, where $\widetilde{E}_{\mathrm{M}}(t)$ is a slow function of time and ω_{M} is the carrier frequency of the microwave field. The higher microwave harmonics, which could also propagate in the loop, but may be filtered, are suppressed. The carrier frequency of the microwave field is expected to be nearly equal to the free spectral range of the optical cavity

$$\omega_{\mathrm{M}}(\tau_{\mathrm{c}}+\tau_{\mathrm{B}})=2\pi+\omega_{\mathrm{M}}\Delta\tau_{\mathrm{c1}},\quad \omega_{\mathrm{M}}\Delta\tau_{\mathrm{c1}}\ll 1. \tag{4}$$

Equation (3) transforms to

$$\tau_{\mathrm{M}}(t)=\tau_{\mathrm{c}}\frac{n_0^2}{4(2^{1/2})}r_{\mathrm{eff}}\left[E_{\mathrm{M}}(t)\exp\left(-\mathrm{i}\frac{\omega_{\mathrm{M}}\Delta\tau_{\mathrm{c1}}}{4}\right)+E_{\mathrm{M}}^{*}(t)\exp\left(\mathrm{i}\frac{\omega_{\mathrm{M}}\Delta\tau_{\mathrm{c1}}}{4}\right)\right]\mathrm{sinc}\frac{\omega_{\mathrm{M}}\Delta\tau_{\mathrm{c1}}}{4}, \tag{5}$$

where $\mathrm{sinc}\,\phi\equiv\sin\phi/\phi$. It is convenient to introduce a dimensionless coupling constant that describes the modulation

$$g=\omega_0\frac{n_0^2}{4(2^{1/2})}r_{\mathrm{eff}}\exp\left(-\mathrm{i}\frac{\omega_{\mathrm{M}}\Delta\tau_{\mathrm{c1}}}{4}\right)\mathrm{sinc}\left(\frac{\omega_{\mathrm{M}}\Delta\tau_{\mathrm{c1}}}{4}\right)E_{\mathrm{M}}, \tag{6}$$

where $E_{\mathrm{M}}=[2\pi\hbar\omega_{\mathrm{R}}/(n_{\mathrm{M}}^2V_{\mathrm{M}})]^{1/2}$ is the field per microwave photon, ω_{R} is the resonance frequency of the microwave resonator, n_{M} is the index of refraction of $LiNbO_3$ at the microwave frequency and V_{M} is the effective volume of the microwave mode; then $\tau_{\mathrm{M}}=\tau_{\mathrm{c}}(gE_{\mathrm{M}}+g^{*}E_{\mathrm{M}}^{*})/(\omega_0E_{\mathrm{M}})$.

To find the output, E_{out}, and feedback, E_4, fields given by

$$E_{\mathrm{out}}(t)=-E_2(t)(1-T_2)^{1/2}-E_3(t)T_2^{1/2}, \tag{7}$$

$$E_4(t)=E_2(t)T_2^{1/2}-E_3(t)(1-T_2)^{1/2}, \tag{8}$$

we note that the electric field after the first delay line, L_1, is

$$E_2(t)=-E_{\mathrm{in}}(t-\tau_1)(1-T_1)^{1/2}-\hat{e}_{\mathrm{d1}}(t-\tau_1)T_1^{1/2}, \tag{9}$$

where $\tau_1=L_1n_{\mathrm{f}}/c$ is the delay time after light propagation in a fibre with length L_1 and n_{f} is the refractive index of the fibre. The electric field after the modulator, E_3, is given by

$$E_3(t)=E_0(t)T_{\mathrm{c2}}^{1/2}-\hat{e}_{\mathrm{d2}}(t)(1-T_{\mathrm{c2}})^{1/2}. \tag{10}$$

The feedback field E_4 is sent through a fibre delay line at the output of which we have

$$E_5(t)=E_4(t-\tau_2), \tag{11}$$

where $\tau_2 = L_2 n_f/c$ is the delay time due to light propagation in a fibre with length L_2. The delayed light then becomes incident on a fast photodiode. The resulting photocurrent is filtered, amplified and sent into the microwave resonator. The electric field at the entrance of the resonator is

$$E_6(t) = \int_{\infty}^{\infty} G(t,t')\left|E_5(t')\right|^2 \mathrm{d}t' + \hat{e}_G(t)\ , \tag{12}$$

where $G(t',t)$ is an effective transmission function of the photodiode, filter and amplifier.

Finally, the electric field inside the microwave resonator obeys the equation

$$E_M(t) = E_6(t)T_M^{1/2} + E_M(t-\tau_R)(1-T_M)^{1/2} - \mathrm{i}g^*\tau_R E_M \frac{\left|E_0(t)\right|^2}{E_0^2}, \tag{13}$$

where T_M is the effective energy transmission coefficient for the resonator, τ_R is the microwave effective roundtrip time in the resonator, $E_0 = [2\pi\hbar\omega_0/(n_0^2 V_0)]^{1/2}$ is the field per optical photon and V_0 is the whispering gallery mode volume.

The last term in equation (13) is the feedback term which appears due to the nonlinear interaction of the microwave field with light. To specify this term we use an approximate interaction Hamiltonian $H = \hbar E_0^2(gE_M + g^*E_M^*)/E_0^2 E_M$ for the microwave field and light, where we assume that the optical cavity modes are nearly equivalent.

Equations (1), (2), (7)–(13) describe the behaviour of the system shown in figure 1. In the following section we discuss their solutions.

2.2. *Solution: expectation values*

To find the solutions for the expectation values and threshold of the oscillation we first solve equation (2) assuming that $E_M(t)$ is a given function of time. We introduce slow amplitudes for the electric fields as $E_j(t) = \widetilde{E}_j(t)\exp(-\mathrm{i}\omega_0 t)$ and, then,

$$\begin{aligned}\widetilde{E}_0(t) = {} & \widetilde{E}_1(t)T_{c1}^{1/2} + \exp\left[\mathrm{i}\omega_0(\tau_c + \tau_B + \tau_M(t))\right] \\ & \times \widetilde{E}_0(t - \tau_c - \tau_B - \tau_M(t))(1 - T_{c1} - T_{c2})^{1/2},\end{aligned} \tag{14}$$

The field inside the cavity $\widetilde{E}_0$ may contain different harmonics with $\pm k\omega_M$, where k is an integer number.

$$\widetilde{E}_0(t) \equiv \sum_k \widetilde{E}_{0k}(t)\ \exp(-\mathrm{i}k\omega_M t), \tag{15}$$

where $E_{0k}(t)$ are slow functions of time. Taking into account equation (4), we introduce an approximation

$$\widetilde{E}_0(t - \tau_c - \tau_B - \tau_M(t)) \approx \widetilde{E}_0(t). \tag{16}$$

This approximation, valid if $\omega_M(\Delta\tau_{c1} + \tau_M(t)) \ll 1$, is equivalent to the steady-state solution of an infinite set of equations for the cavity modes which may be derived from equation (2).

It is convenient to introduce a detuning parameter $\Delta\tau_{c2}$ for the cavity mode pumped by the laser (cf. equation (4))

$$\omega_0(\tau_c + \tau_B) = 2\pi\nu + \omega_0\Delta\tau_{c2}, \quad \omega_0\Delta\tau_{c2} \ll 1, \tag{17}$$

where ν is the mode number. Then, taking into account equation (1), we arrive at

$$E_0(t) \approx \frac{2E_{\rm in}(t)\,(T_1 T_{\rm c1})^{1/2}}{T_{\rm c1} + T_{\rm c2} - 2{\rm i}\omega_0(\Delta\tau_{\rm c2} + \tau_{\rm M}(t))}. \tag{18}$$

Equation (18) is valid even for $\omega_0\tau_{\rm M}(t) \gg T_{\rm c1} + T_{\rm c2}$.

For the sake of simplicity, we assume that $T_{\rm c1} = T_{\rm c2} = T_{\rm c}$, $T_1 = T_2 = 1/2$ and $E_{\rm in}(t - \tau_1) = {\rm i}E_{\rm in}(t)$. This choice maximizes the resultant amplitude modulation signal in the feedback loop. It is now easy to find

$$E_5(t) = -\frac{E_{\rm in}(t)}{2}\exp({\rm i}\omega_0\tau_2)\left[\frac{{\rm i} + 1 + (\omega_0/T_{\rm c})\,(\Delta\tau_{\rm c2} + \tau_{\rm M}(t-\tau_2))}{1 - {\rm i}\,(\omega_0/T_{\rm c})\,(\Delta\tau_{\rm c2} + \tau_{\rm M}(t-\tau_2))}\right]. \tag{19}$$

While the total optical energy is incident on the photodetector, we are interested in the part of the microwave radiation emerging from the photodiode that is resonant with the mode of the microwave resonator. So we use the following transmission function for the diode–filter–amplifier chain:

$$E_6(t) \simeq G\gamma_G \int_0^t {\rm d}t' \exp[-(\gamma_G + {\rm i}\omega_{\rm M})(t - t')]P_5(t'), \tag{20}$$

where $P_5(t)$ is the power of the incident light and $\gamma_G \ll \omega_{\rm M}$ is the filter bandwidth. The feedback microwave field may be estimated as

$$\begin{aligned} E_6(t) \approx G\gamma_G \frac{P_{\rm in}}{4}\int_0^t {\rm d}t' \exp[-(\gamma_G + {\rm i}\omega_{\rm M})(t - t')] \\ \times \frac{1 + (1 + (\omega_0/T_{\rm c})\,\widetilde{\tau}_{\rm M}(t-\tau_2)\cos(\omega_{\rm M}(t' - \Delta\tau_2) + \psi))^2}{1 + (\omega_0/T_{\rm c})^2\,\widetilde{\tau}^2_{\rm M}(t-\tau_2)\cos^2(\omega_{\rm M}(t' - \Delta\tau_2) + \psi)}, \end{aligned} \tag{21}$$

where we have introduced $\tau_{\rm M}(t) = \widetilde{\tau}_{\rm M}(t)\cos(\omega_{\rm M}t + \psi)$, and assumed that

$$\omega_{\rm M}\tau_2 = 2\pi m + \omega_{\rm M}\Delta\tau_2, \quad \omega_{\rm M}\Delta\tau_2 \ll 1. \tag{22}$$

Here m is an integer number, $P_{\rm in}$ is the incident optical power and G is the effective transformation coefficient which takes into account the response of the photodiode, filter and amplifier. We have also neglected the term $\Delta\tau_{\rm c2}$ and assumed that the light field is nearly resonant with the optical cavity modes. Equation (21) may be reduced to

$$\begin{aligned} E_6(t) = G\frac{P_{\rm in}}{2}\exp[-{\rm i}(\omega_{\rm M}(t - \Delta\tau_2) + \psi)] \\ \times \left[\frac{[1 + (\omega_0/T_{\rm c})^2\,\widetilde{\tau}^2_{\rm M}(t-\tau_2)]^{1/2} - 1}{(\omega_0/T_{\rm c})\,\widetilde{\tau}_{\rm M}(t-\tau_2)\,[1 + (\omega_0/T_{\rm c})^2\,\widetilde{\tau}^2_{\rm M}(t-\tau_2)]^{1/2}}\right]. \end{aligned} \tag{23}$$

To solve equation (13) we have to find the resonant part of the term containing $|E_0(t)|^2$. This term does not contribute significantly to the field amplification.

However, it influences the frequency of the oscillation. We note that

$$\left|E_0(t)\right|^2\big|_{\omega_M} = \frac{|E_{in}|^2}{2T_c}\frac{\omega_M}{2\pi} \times \int_0^{2\pi/\omega_M} \frac{\exp[i\omega_M(t'-t)]dt'}{1+(\omega_0/T_c)^2(\Delta\tau_{c2}+\widetilde{\tau}_M(t)\cos(\omega_M t'+\psi))^2} + c.c.$$
$$\approx -\frac{|E_{in}|^2}{2T_c}\frac{\widetilde{\tau}_M(t)\exp[-i(\omega_M t+\psi)]\Delta\tau_{c2}(\omega_0/T_c)^2}{(1+(\omega_0/T_c)^2\widetilde{\tau}_M^2(t))^{3/2}} + c.c., \tag{24}$$

where we kept terms linear in $\Delta\tau_{c2}$.

Finally, assuming that

$$\omega_M\tau_R = 2\pi + \omega_M\Delta\tau_R, \quad \omega_M\Delta\tau_R \ll 1, \tag{25}$$

we can solve equation (13) in the steady state. The equation for the field amplitude is

$$2g\tau_c\frac{|E_M|^2}{E_M G P_{in}}\frac{T_M^{1/2}}{T_c} = 1 - \left[1+\left(\frac{2g\tau_c|E_M|}{T_c E_M}\right)^2\right]^{-1/2}. \tag{26}$$

To simplify this expression we assume that the saturation is small, i.e. $1 \gg 2g\tau_c|E_M|/(T_c E_M)$ and derive

$$|E_M|^2 = \left|\frac{T_c E_M}{3^{1/2} g\tau_c}\right|^2 \left(1 - \frac{T_M^{1/2} T_c E_M}{g\tau_c G P_{in}}\right). \tag{27}$$

This equation allows us to find the threshold pump power for the oscillation:

$$P_{th} = \frac{4(2^{1/2})T_M^{1/2}T_c}{G\omega_0\tau_c n_0^2 r_{eff}} = \frac{8\pi^{1/2}}{GQ_0Q_M^{1/2}n_0^2 r_{eff}}. \tag{28}$$

To estimate the saturated value of the amplitude of the microwave field we assume that $2g\tau_c|E_M|/(T_c E_M) \gg 1$ and find

$$|E_{Msat}|^2 \approx \frac{2(2^{1/2})T_c G P_{in}}{\omega_0\tau_c n_0^2 r_{eff} T_M^{1/2}} = \frac{2}{\pi^{1/2}}\frac{GP_{in}}{n_0^2 r_{eff}}\frac{Q_M^{1/2}}{Q_0}, \tag{29}$$

where Q_0 and Q_M are the quality factors of the optical cavity and the microwave resonator, respectively.

The oscillation frequency is determined by the equation

$$\Delta\tau_R = -\frac{T_M}{2}\left(\Delta\tau_2 - \frac{\Delta\tau_{c1}}{4}\right) - \Delta\tau_{c2}\frac{1}{T_c}\frac{g^2\tau_c^2}{T_c^2}\frac{|E_{in}|^2}{E_0^2}\frac{\omega_0}{\omega_M}, \tag{30}$$

where we have assumed that $\tau_M \simeq \tau_c$ and ω_c is the frequency of the optical cavity mode. Since the feedback delay time is much larger than the cavity roundtrip time ($\tau_2 \gg \tau_c$), we rewrite equation (30) in the form

$$\omega_M - \omega_R = -\frac{T_M}{2}\frac{\tau_2}{\tau_c}(\omega_M - \omega_{L2}) - \frac{1}{T_c}\frac{g^2\tau_c^2}{T_c^2}\frac{|E_{in}|^2}{E_0^2}\left(\omega_0 - \omega_c\frac{\tau_c}{\tau_c+\tau_B}\right), \tag{31}$$

where ω_{L2} is the microwave frequency determined by the delay line L_2. Therefore, the oscillation frequency is determined by the competition of two microwave

resonances and is influenced by the tuning of the optical pump. The nonlinear term may be compensated for by proper tuning of the laser frequency, or by applying a DC bias to the electro-optic resonator. In the following we show that this coupling results in the noise contamination of the microwave signal by the phase diffusion of the optical field.

Let us make numerical estimations for the system. We note that $T_M/(2\tau_c) = \gamma_M$ is the linewidth of the microwave resonator, and $\omega_M/(2\gamma_M) = Q_M$ is the quality factor of the resonator. Under the usual experimental conditions it is possible to achieve $Q_M = 100$. For microwave frequency $\omega_M = 2\pi \times 10^{10}\,\mathrm{rad\,s^{-1}}$ we have $\gamma_M = \pi \times 10^8\,\mathrm{rad\,s^{-1}}$, $\tau_c = 2\pi/\omega_M = 10^{-10}\,\mathrm{s}$ and $T_M = 2\pi \times 10^{-2}$.

Similarly, for the optical cavity, $T_c/(2\tau_c) = \gamma$ is the linewidth of the cavity and $\omega_c/(2\gamma) = Q$ is the quality factor of the cavity. With the lithium niobate optical cavity it is possible to achieve $Q = 10^7$. For the optical frequency $\omega_0 = 2\pi \times 2 \times 10^{14}\,\mathrm{rad\,s^{-1}}$ we have $\gamma = 2\pi \times 10^7\,\mathrm{rad\,s^{-1}}$ and $T_c = 2\pi \times 10^{-3}$.

With a $L_2 = 1$ km fibre the delay time is approximately $\tau_2 \simeq 5 \times 10^{-6}\,\mathrm{s}$. Hence $T_M\tau_2/2\tau_c \simeq 1600$ and the microwave frequency is dictated by the delay line instead of the microwave resonator.

To find the coupling constant g we first estimate the amplitude of electric field per microwave photon E_M. The volume of the microwave field is $V_M \approx 10^{-4}\,\mathrm{cm^3}$, and the microwave susceptibility of $LiNbO_3$ is $n_M^2 = 29$; hence, $E_M \approx 3.7 \times 10^{-7}$ CGS. The maximum electro-optic constant for $LiNbO_3$ is $r_{eff} = r_{33} = 30\,\mathrm{pmV^{-1}} = 9 \times 10^{-7}$ CGS. The index of refraction for $LiNbO_3$ is $n_0 = 2.14$. Using the above values we arrive at $g \approx 300\,\mathrm{s^{-1}}$.

The coefficient of conversion of light energy into microwave oscillation by means of a photodiode may be determined from the expression $P_{mW} = \mathcal{R}^2\rho P_{opt}^2$, where $\mathcal{R} = 0.7\ \mathrm{A\,W^{-1}}$ and $\rho = 50\Omega$. Let us assume that the amplifier is switched off, then $G = \mathcal{R}(2\pi\rho/\mathcal{A}_M c)^{1/2} \approx 7 \times 10^{-7}$ CGS, where $\mathcal{A}_M \approx 10^{-4}\,\mathrm{cm^2}$ is the cross-sectional area of the microwave waveguide mode. Therefore, the threshold optical power is approximately $P_{th} \approx 2$ mW. With additional electrical amplification of the signal in the feedback loop, this value may be further reduced.

Finally, let us find the nonlinear coupling coefficient in the equation for the microwave frequency. We note that $|E_{in}|^2 = 2\pi P_{in}/\mathcal{A}c \approx 10^2$ CGSE for $P_{in} = 10\,\mathrm{mW} = 10^5\,\mathrm{CGSE}$ and $\mathcal{A} = 2 \times 10^{-7}\,\mathrm{cm^2}$. The electric field per optical photon is $E^2 = 2\pi\hbar\omega_0/V_0 n_0^2 \approx 2 \times 10^{-6}\,\mathrm{CGSE}$, for $V_0 = 6 \times 10^{-7}\,\mathrm{cm^3}$. Under these conditions the nonlinear coupling constant in front of $\omega_0 - \omega_c$ (see equation (31)) is equal to 0.2.

2.3. *Solution: fluctuations*

To produce the condition for stable oscillation the OEO should work at a weak modulation regime. This is because near the saturation point, the modulator converts the phase fluctuations of the pump laser to amplitude fluctuations, and vice versa, thereby increasing the overall noise. The weak modulation regime is characterized by condition $T_{c1} + T_{c2} \gg 2\omega_0\tau_M(t)$ at any time t.

To avoid the conversion of the laser phase noise to amplitude noise the laser must be tuned to the centre of an optical resonance. Fine tuning of the laser carrier frequency and the DC bias field allows fulfilling this condition and achieving $\Delta\tau_{c2} \to 0$.

We present the electric field at the input of the system, and the microwave field as

$$E_{\mathrm{in}}(t) = \{[|\langle E_{\mathrm{in}}\rangle| + \delta e_{\mathrm{in}}(t)]\exp[-\mathrm{i}\phi_{\mathrm{in}} - \mathrm{i}\delta\phi_{\mathrm{in}}(t)] + \tilde{\hat{e}}_{\mathrm{in}}(t)\}\exp(-\mathrm{i}\omega_0 t), \tag{32}$$

$$E_{\mathrm{M}}(t) = \{[|\langle E_{\mathrm{M}}\rangle| + \delta e_{\mathrm{M}}(t)]\exp[-\mathrm{i}\phi_{\mathrm{M}} - \mathrm{i}\delta\phi_{\mathrm{M}}(t)] + \tilde{\hat{e}}_{\mathrm{M}}(t)\}\exp(-\mathrm{i}\omega_{\mathrm{M}} t), \tag{33}$$

where $|\langle E_{\mathrm{in}}\rangle|$ and ϕ_{in} are averaged field amplitudes and phase, and $\delta e_{\mathrm{in}}(t)$ and $\delta\phi_{\mathrm{in}}(t)$ are the classical amplitude and phase counterparts of the laser noise, ω_0 is the carrier frequency. Similarly, $|\langle E_{\mathrm{M}}\rangle|$ and ϕ_{M} are averaged microwave amplitude and phase, $\delta e_{\mathrm{M}}(t)$ and $\delta\phi_{\mathrm{M}}(t)$ are the classical microwave amplitude and phase noise, ω_{M} is the carrier microwave frequency, $\tilde{\hat{e}}_{\mathrm{in}}(t)$ and $\tilde{\hat{e}}_{\mathrm{M}}(t)$ are the quantum parts of the fluctuations (tilde here indicates that the spectrum of the fluctuations is considered relative to the line centre). We assume that the quantum part of the fluctuations is wide band noise, while the classical fluctuations are narrow band noise, i.e. they have a bandwidth much narrower than the free spectral range of the optical cavity.

The optical cavity field may be presented in the form

$$E_0(t) \approx \frac{1}{2^{1/2}}\frac{(\tilde{E}_{\mathrm{in}}(t-\tau_{\mathrm{c}}/T_{\mathrm{c}}) - \tilde{\hat{e}}_{\mathrm{d1}}(t-\tau_{\mathrm{c}}/T_{\mathrm{c}}))\exp(-\mathrm{i}\omega_0 t)T_{\mathrm{c}}^{1/2}}{T_{\mathrm{c}} - \mathrm{i}(\omega_0\tau_{\mathrm{M}}(t) + 2\pi\delta\dot{\phi}_{\mathrm{in}}(t)/\omega_{\mathrm{M}})}$$

$$+ \frac{\tilde{\hat{e}}_{\mathrm{d2}}(t)\exp(-\mathrm{i}\omega_0 t)T_{\mathrm{c}}^{1/2}}{T_{\mathrm{c}} - \mathrm{i}(\omega_0\tau_{\mathrm{M}}(t) + 2\pi\delta\dot{\phi}_{\mathrm{in}}(t)/\omega_{\mathrm{M}})}, \tag{34}$$

where $\tilde{E}_{\mathrm{in}}(t-\tau_{\mathrm{c}}/T_{\mathrm{c}})$ and $\tilde{\hat{e}}_{\mathrm{d1}}(t-\tau_{\mathrm{c}}/T_{\mathrm{c}})$ are the slow field amplitudes, $\tau_{\mathrm{c}}/T_{\mathrm{c}}$ stands for the group delay and $\delta\dot{\phi}_{\mathrm{in}}(t)$ results from the phase diffusion of the pump laser. Equation (34) was derived under the assumption of unsaturated modulation, $T_{\mathrm{c}} \gg \omega_0\tau_{\mathrm{M}}(t)$, and small phase diffusion of the pump laser, $T_{\mathrm{c}} \gg 2\pi\delta\dot{\phi}_{\mathrm{in}}(t)/\omega_{\mathrm{M}}$. For the saturated case and/or large phase diffusion the modulator transforms the phase fluctuations of the laser to the amplitude fluctuations.

Because the optical cavity introduces a group delay, the scheme may transfer the phase fluctuations of the laser into the amplitude of the transmitted light. These fluctuations simply do not cancel each other on the beam splitter T_2. To avoid this transfer effect one needs to choose the delay time of the interferometer arm without a cavity such that $\tau_1 = \tau_{\mathrm{c}}/T_{\mathrm{c}}$. For simplicity reasons we also assume that $\exp(-\mathrm{i}\omega_0\tau_1) = \mathrm{i}$. Generally, such a balance of the interferometer is not critical. The difference between τ_1 and $\tau_{\mathrm{c}}/T_{\mathrm{c}}$ should be much less than the inverse pump laser linewidth. If the laser linewidth is narrow enough, no balancing is necessary.

In the limit of small modulation the electric field of light at the output of the delay line L_2 is

$$E_5(t) \simeq -\frac{\mathrm{i}-1}{2}\hat{e}_{\mathrm{d1}}(t) - \frac{E_{\mathrm{in}}(t)}{2}\exp(\mathrm{i}\omega_0\tau_2)$$

$$\times\left[\frac{\mathrm{i}+1+(2\pi\delta\dot{\phi}_{\mathrm{in}}(t-\tau_2)/\omega_{\mathrm{M}} + \omega_0\tau_{\mathrm{M}}(t-\tau_2))/T_{\mathrm{c}}}{1-\mathrm{i}(2\pi\delta\dot{\phi}_{\mathrm{in}}(t-\tau_2)/\omega_{\mathrm{M}} + \omega_0\tau_{\mathrm{M}}(t-\tau_2))/T_{\mathrm{c}}}\right], \tag{35}$$

where some unimportant time delays were omitted. Vacuum fluctuation $\hat{e}_{\mathrm{d2}}(t)$ resulting from the second beam splitter does not contribute to the field.

The microwave field at the input of the microwave resonator is given by

$$E_6(t) \simeq G\gamma_G \frac{P_{\rm in}}{2^{1/2}} \int_0^t {\rm d}t' \exp[-(\gamma_G + {\rm i}\omega_{\rm M})(t-t')] \frac{\tilde{\hat{e}}_5(t') + \tilde{\hat{e}}_5^{\dagger}(t')}{|\langle E_{\rm in}\rangle|} + G\frac{P_{\rm in}}{2}\left(1 + \frac{\delta e_{\rm in} + \delta e_{\rm in}^*}{|\langle E_{\rm in}\rangle|}\right) \times \frac{g\tau_{\rm c} E_{\rm M}(t-\tau_2)}{T_{\rm c} E_{\rm M}} \left[1 - \left(\frac{3^{1/2} g\tau_{\rm c}|E_{\rm M}(t-\tau_2)|}{T_{\rm c} E_{\rm M}}\right)^2\right] + G_a\,\hat{e}_6(t) + (G_a^2 - 1)^{1/2}\,\hat{e}_G^{\dagger}(t). \tag{36}$$

where $\hat{e}_5(t) = (\hat{e}_{\rm in}(t) - [(1-{\rm i})/(1+{\rm i})]\,\hat{e}_{\rm d1}(t))/2^{1/2}$ describes vacuum fluctuations of the field $E_5(t)$. Equation (36) consists of three parts. The first part describes the shot noise on the photodetector which results from vacuum fluctuations of light. In deriving this term we neglected the modulation of light. The second part contains the expectation for the value of the microwave field in the feedback loop as well as the narrow band classical amplitude noise of the pump laser. Finally, the third part results from the noise of the photodetector and the amplifier. The term $\hat{e}_6(t)$ describes vacuum quantum fluctuations of the running electromagnetic wave, and $G_a \geq 1$ shows the noise increase due to the amplifier and the photodiode. The term $\hat{e}_G(t)$ stands for the amplifier and photodetector noise. The parameter G_a always exceeds the power amplification coefficient of the amplifier.

We note that the power of the cavity field is modulated on the microwave frequency when there exists a non-zero phase diffusion of the pump laser radiation. Using equation (34) we find

$$|E_0(t)|^2|_{\omega_{\rm M}} = -\frac{|\langle E_{\rm in}\rangle|^2}{2T_{\rm c}}\tilde{\tau}_{\rm M}(t)\,\exp[-{\rm i}(\omega_{\rm M} t + \psi)]\frac{2\pi\delta\dot{\phi}_{\rm in}(t)}{\omega_0\omega_{\rm M}}\left(\frac{\omega_0}{T_{\rm c}}\right)^2 + c.c., \tag{37}$$

keeping terms linear in fluctuations only. Generally, this expression implies that even small detuning of the laser frequency from the exact overlap with a cavity mode frequency results in amplitude modulation of laser radiation. In our case this effect influences the OEO stability.

Let us now find the phase diffusion for the microwave field generated in the OEO. We solve equation (13) in steady state for the expectation values of the microwave field amplitude and frequency, which is equivalent to the solution of equations (26) and (31). The phase fluctuations of the microwaves obeys the equation:

$$-\delta\dot{\phi}_{\rm M}(t)|\langle E_{\rm M}\rangle|\left(\tau_{\rm R} + \frac{T_{\rm M}}{2}\tau_2\right) = T_{\rm M}^{1/2}\left[-G\gamma_G\frac{P_{\rm in}}{2^{1/2}} \times \int_0^t {\rm d}t' \exp[-\gamma_G(t-t')]\sin(\omega_{\rm M}t')\frac{\tilde{\hat{e}}_5(t') + \tilde{\hat{e}}_5^{\dagger}(t')}{|\langle E_{\rm in}\rangle|} - \frac{{\rm i}G_a}{2}(\hat{e}_6 - \hat{e}_6^{\dagger}) + \frac{{\rm i}(G_a^2-1)^{1/2}}{2}(\hat{e}_G - \hat{e}_G^{\dagger})\right] + |\langle E_{\rm M}\rangle|\frac{|g|^2\tau_{\rm c}^2}{T_{\rm c}^2}\frac{|\langle E_{\rm in}\rangle|^2}{E_0^2}\frac{2\pi\delta\dot{\phi}_{\rm in}}{T_{\rm c}\omega_{\rm M}}. \tag{38}$$

Introducing phase diffusion coefficient D as $\langle\delta\phi(t)^2\rangle - \langle\delta\phi(t)\rangle^2 = 2Dt$ and assuming that the time of the measurement is much longer than the filter characteristic time

$1/\gamma_G$ we arrive at

$$D_{\mathrm{M}} = \tilde{\gamma}_{\mathrm{M}}^2 \frac{\hbar\omega_{\mathrm{M}}}{2P_{M_{\mathrm{out}}}} \left(2G_a^2 - 1 + \left(\frac{G}{2\pi}\right)^2 \omega_0 V_{\mathrm{M}} P_{\mathrm{in}} \right) + \left(\frac{2\tau_{\mathrm{c}}}{2\tau_{\mathrm{c}} + T_{\mathrm{M}}\tau_2} \frac{|g|^2\tau_{\mathrm{c}}^2}{T_{\mathrm{c}}^3} \frac{|\langle E_{\mathrm{in}}\rangle|^2}{E_0^2} \right)^2 D_{\mathrm{in}}, \tag{39}$$

where $\tilde{\gamma}_{\mathrm{M}} = T_{\mathrm{M}}/(2\tau_{\mathrm{c}} + T_{\mathrm{M}}\tau_2)$ is the effective decay rate of the microwave cavity and D_{in} is the phase diffusion of the input laser. Equation (39) indicates that the oscillator is closer to the Shawlow–Townes limit for smaller P_{in}.

The above analysis is valid for an unsaturated modulator, $P_{\mathrm{th}} \geq P_{\mathrm{in}} \geq 2P_{\mathrm{th}}$, where P_{th} can be found from equation (28). We estimate

$$D_{\mathrm{M}} \approx \frac{\tilde{\gamma}_{\mathrm{M}}^2}{2} \left(\frac{2\pi}{Q_{\mathrm{M}}}\right)^{1/2} \frac{\hbar\omega_0}{P_{\mathrm{th}}} \left[1 + \frac{8\pi^2(2G_a^2 - 1)}{G^2 P_{\mathrm{th}} V_{\mathrm{M}} \omega_0} \frac{P_{\mathrm{th}}}{P_{\mathrm{in}}} \right] + \left(\frac{2\tau_{\mathrm{c}} T_{\mathrm{M}}}{n_{\mathrm{M}}^2 T_{\mathrm{c}}(2\tau_{\mathrm{c}} + T_{\mathrm{M}}\tau_2)} \frac{P_{\mathrm{in}}}{P_{\mathrm{th}}} \frac{8\pi^2}{G^2 P_{\mathrm{th}} V_{\mathrm{M}} \omega_0} \right)^2 D_{\mathrm{in}}. \tag{40}$$

For the parameters indicated above and $\tau_2 = 2 \times 10^{-5}$ s, $P_{\mathrm{in}}/P_{\mathrm{th}} = 2$, we derive $D_{\mathrm{M}} \approx 2 \times 10^{-8}(1 + 0.034(2G_a^2 - 1))\mathrm{s}^{-1} + 10^{-12} D_{\mathrm{in}}$.

Finally, it worth noting that the spectral density of the microwave frequency fluctuations is constant in the approximations made above. The ratio of quadratic deviation of the oscillation frequency averaged during time t and the average frequency (Allen deviation) is

$$\frac{\sigma_{\omega_{\mathrm{M}}}}{\omega_{\mathrm{M}}} = \left(\frac{2D_{\mathrm{M}}}{t\omega_{\mathrm{M}}^2}\right)^{1/2}. \tag{41}$$

For the above estimations $\sigma_{\omega_{\mathrm{M}}}/\omega_{\mathrm{M}} \simeq 3 \times 10^{-15}/t^{1/2}$.

3. Non-resonant optoelectronic oscillator

In this section we recall the properties of the non-resonant OEO described previously in [1]. We derive expressions for the oscillation threshold, oscillation frequency and noise of the oscillator.

3.1. *Basic equations*

Let us consider the OEO scheme shown in figure 2. An efficient modulation is possible only if the phase matching condition for light and microwaves is established in a planar sample of an electro-optic material. This can be achieved, for example, if one uses periodically poled nonlinear crystals and polymers [7, 20, 21], or planar microstrip microwave waveguide [22–24].

Equations (1), (7)–(9), (11) and (12) hold for the scheme. Instead of equations (2) and (10) we write the equation

$$E_3(t) = E_1(t - \tau_{\mathrm{B}} - \tau_{\mathrm{M}}(t)). \tag{42}$$

The time varying delay may be presented as (cf. equations (3) and (5))

$$\tau_{\mathrm{M}}(t) = \xi\tau_{\mathrm{S}} \frac{n_0^2}{2} r_{\mathrm{eff}}(E_{\mathrm{M}}(t) + E_{\mathrm{M}}^*(t)), \tag{43}$$

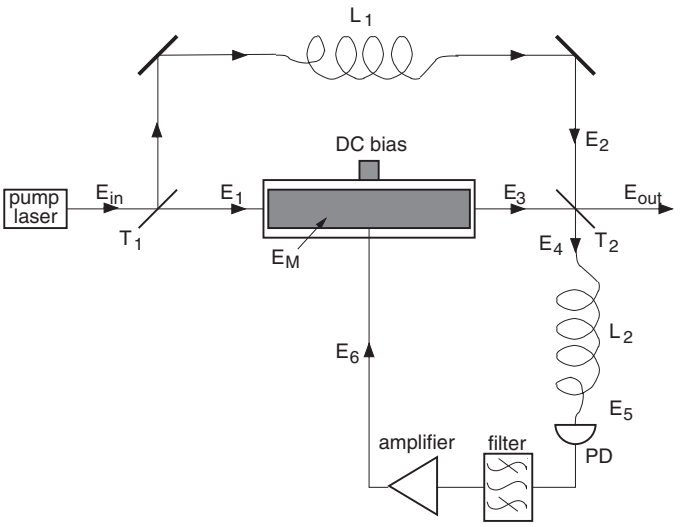

Figure 2. Opto-electronic oscillator based on a planar $LiNbO_3$ electro-optic modulator.

where $\tau_S = L_S n_0/c$ is the propagation time of light in the $LiNbO_3$ crystal, L_S is the crystal length and $\xi < 1$ results from imperfect overlap and phase mismatch of the light and the microwave fields.

Finally, instead of equation (13) we write

$$E_M(t) = E_6(t). \tag{44}$$

Here, there are no nonlinear terms proportional to the light power because only the phase of light is modulated in the nonlinear crystal; the power of light inside the crystal stays unchanged ($|E_3(t)|^2|_{\omega_M} = 0$).

3.2. *Solution: expectation values*

Assuming that $T_1 = T_2 = 1/2$ we derive

$$E_3(t) = \frac{1}{2^{1/2}} E_{in}(t) \exp[i\omega_0(\tau_B + \tau_M(t))]. \tag{45}$$

On the other hand

$$E_2(t) = -\frac{1}{2^{1/2}} E_{in}(t) \exp(i\omega_0\tau_1). \tag{46}$$

From equation (8) we derive

$$E_4(t) = -\frac{1}{2} E_{in}(t) \exp(i\omega_0\tau_1)(1 + \exp[i\omega_0(\tau_B - \tau_1 + \tau_M(t))]). \tag{47}$$

The power of the field $E_5(t)$ is, therefore,

$$P_5(t) = \frac{P_{in}}{2}[1 + \cos\omega_0(\tau_B - \tau_1 + \tau_M(t - \tau_2))]. \tag{48}$$

The microwave field may be determined from equation

$$E_{\mathrm{M}}(t) \approx G\gamma_G \frac{P_{\mathrm{in}}}{2} \int_0^t \mathrm{d}t' \exp[-(\gamma_G + \mathrm{i}\omega_{\mathrm{M}})(t-t')]$$
$$\times \cos\omega_0[\tau_{\mathrm{B}} - \tau_1 + \widetilde{\tau}_{\mathrm{M}}(t-\tau_2)\cos(\omega_{\mathrm{M}}(t'-\Delta\tau_2) + \psi)]$$
$$= -G\frac{P_{\mathrm{in}}}{2}\exp[-\mathrm{i}(\omega_{\mathrm{M}}(t-\Delta\tau_2) + \psi)]$$
$$\times \sin[\omega_0(\tau_{\mathrm{B}} - \tau_1)]J_1[\omega_0\,\widetilde{\tau}_{\mathrm{M}}(t-\tau_2)], \tag{49}$$

where, as above, we have introduced $\tau_{\mathrm{M}}(t) = \widetilde{\tau}_{\mathrm{M}}(t)\cos(\omega_{\mathrm{M}}t + \psi)$ and assumed that condition (22) is fulfilled (however, we do not demand here that $\omega_{\mathrm{M}}\Delta\tau_2 \ll 1$). $J_1[...]$ is the Bessel function.

Assuming that $\omega_0\,\widetilde{\tau}_{\mathrm{M}}(t-\tau_2) \ll 1$ and decomposing the Bessel function into a Taylor series ($J_1(x) \approx x/2 - (1/2)(x/2)^3$, if $x \ll 1$) we derive the expression for the microwave field amplitude

$$|E_{\mathrm{M}}|^2 = \frac{8}{(\xi\tau_{\mathrm{S}}\omega_0 n_0^2 r_{\mathrm{eff}})^2}\left[1 - \frac{4\left|\sin[\omega_0(\tau_{\mathrm{B}} - \tau_1)]\right|}{GP_{\mathrm{in}}\xi\tau_{\mathrm{S}}\omega_0 n_0^2 r_{\mathrm{eff}}}\right]. \tag{50}$$

Therefore, the oscillation threshold for the pump light power is

$$P_{\mathrm{th}} = \frac{4}{G\xi\tau_{\mathrm{S}}\omega_0 n_0^2 r_{\mathrm{eff}}}, \tag{51}$$

where we assumed that $|\sin[\omega_0(\tau_{\mathrm{B}} - \tau_1)]| = 1$. One can see that the main difference between equations (28) and (51) results from the high finesse of the cavities. The smaller T_{c} and T_{M} are, the lower is the threshold in the case of the cavity enhanced OEO. No dependence on the mode volume is present.

The difference from the resonance case is the absence of conventional saturation in the non-resonant OEO. Indeed, for $\omega_0\,\widetilde{\tau}_{\mathrm{M}}(t) \gg 1$ we have $J_1[\omega_0\,\widetilde{\tau}_{\mathrm{M}}(t)] \approx (\sin[\omega_0\,\widetilde{\tau}_{\mathrm{M}}(t)] - \cos[\omega_0\,\widetilde{\tau}_{\mathrm{M}}(t)])/[\pi\omega_0\,\widetilde{\tau}_{\mathrm{M}}(t)]^{1/2}$. This function oscillates with the increase of the microwave field amplitude.

The oscillation frequency is to be determined from the equation

$$-\exp(\mathrm{i}\omega_{\mathrm{M}}\Delta\tau_2)\arg(\sin, [\omega_0(\tau_{\mathrm{B}} - \tau_1)]) = 1, \tag{52}$$

resulting in the condition for the oscillation frequency

$$\omega_{\mathrm{M}} = \frac{2\pi m}{\tau_2} + \frac{\pi}{\tau_2}, \quad \text{if } \sin[\omega_0(\tau_{\mathrm{B}} - \tau_1)] > 0;$$
$$\omega_{\mathrm{M}} = \frac{2\pi m}{\tau_2}, \quad \text{if } \sin[\omega_0(\tau_{\mathrm{B}} - \tau_1)] < 0. \tag{53}$$

3.3. *Solution: fluctuations*

Generally, the description of fluctuations of the non-resonant OEO is similar to the description for the resonant one. The microwave field at the input of the

microwave resonator is

$$E_6(t) \simeq G\gamma_G \frac{P_{\rm in}}{2^{1/2}} \int_0^t {\rm d}t' \exp[-(\gamma_G + {\rm i}\omega_{\rm M})(t-t')] \frac{\tilde{\hat{e}}_5(t') + \tilde{\hat{e}}_5^{\dagger}(t')}{|\langle E_{\rm in}\rangle|} + G\frac{P_{\rm in}}{2}\left(1 + \frac{\delta e_{\rm in} + \delta e_{\rm in}^*}{|\langle E_{\rm in}\rangle|}\right) \times \frac{g\tau_{\rm c} E_{\rm M}(t-\tau_2)}{E_{\rm M}} \left[1 - \left(\frac{g\tau_{\rm c}|E_{\rm M}(t-\tau_2)|}{4E_{\rm M}}\right)^2\right] + G_a\,\hat{e}_6(t) + (G_a^2 - 1)^{1/2}\,\hat{e}_G^{\dagger}(t). \tag{54}$$

where $\hat{e}_5(t)$ describes the coherent vacuum fluctuations of the field $E_5(t)$. Equation (54) consists of three parts having the same origin as parts of equation (36). We assumed here that $\sin[\omega_0(\tau_{\rm B} - \tau_1)] = 1$.

The corresponding equation for the phase fluctuations is

$$-\delta\dot{\phi}_{\rm M}(t)|\langle E_{\rm M}\rangle|\tau_2 = -G\gamma_G \frac{P_{\rm in}}{2^{1/2}} \times \int_0^t {\rm d}t' \exp[-\gamma_G(t-t')] \sin(\omega_{\rm M}t') \frac{\tilde{\hat{e}}_5(t') + \tilde{\hat{e}}_5^{\dagger}(t')}{|\langle E_{\rm in}\rangle|} - \frac{{\rm i}G_a}{2}(\hat{e}_6 - \hat{e}_6^{\dagger}) + \frac{{\rm i}(G_a^2 - 1)^{1/2}}{2}(\hat{e}_G - \hat{e}_G^{\dagger}). \tag{55}$$

Therefore, for the phase diffusion we have

$$D_{\rm M} = \frac{1}{\tau_2^2}\frac{\hbar\omega_{\rm M}}{2P_{M_{\rm out}}}\left(2G_a^2 - 1 + \left(\frac{G}{2\pi}\right)^2 \omega_0 V_{\rm M} P_{\rm in}\right).$$

Because the non-resonant system does not saturate for reasonable values of the optical power, the polynomial decomposition of the Bessel function holds, $P_{\rm M}$ increases faster than $P_{\rm in}$, and $D_{\rm M}$ decreases with the optical power increase. The threshold power for the non-resonant oscillations is about 80 mW if there is no amplification in the feedback loop and $\tau_{\rm S} = 5\tau_{\rm c}$ (the length of the nonlinear crystal is five times longer than the circulation length of the WGM in the case of the resonant OEO).

4. Experiment

We have performed preliminary experimental studies of the OEO based on a high-Q WGM electro-optic modulator. The scheme of the OEO is shown in figure 3. At the present stage the OEO is not optimized as in figure 1. Light is sent directly to the photodiode after the modulator. Because the modulation is primarily of the phase type, conversion of the modulated light into microwaves is inefficient, and significant microwave amplification (42 dB) is required to achieve self-sustained oscillation in this set-up. We use a −10 dB optical splitter and a −6 dB microwave splitter to monitor the properties of the generated microwave power and the modulated light. The length of the optical delay line is $L = 1$ km.

The modulator (see in figure 4) is fully integrated with input optics and built on a copper platform. To our knowledge, this is the first example of integration of a high-Q crystal WGM cavity into a photonic device. The performance of the EOM remains stable during weeks of operation and the quality factors of WGMs do not degrade with time. In principle, the size of the platform may be significantly reduced.

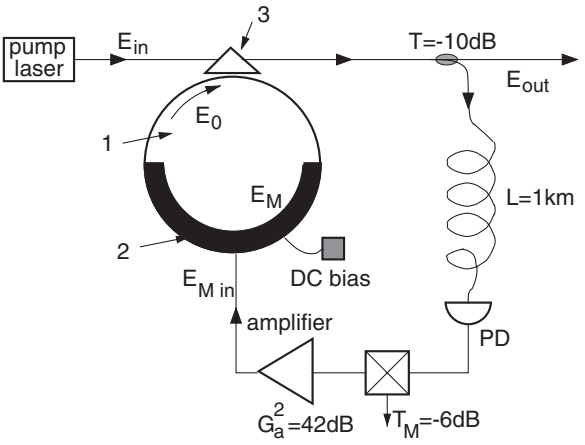

Figure 3. Scheme of the experimentally realized WGM OEO.

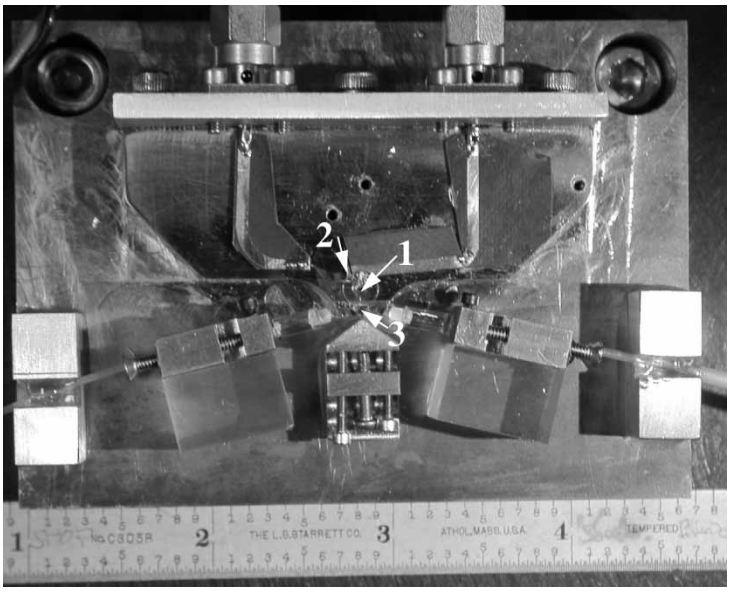

Figure 4. Fully integrated electro-optical modulator based on a whispering gallery mode cavity. The numbers stand for: (1) the WGM cavity, (2) the microstrip microwave resonator and (3) the coupling prism (cf. figure 3).

Because the general properties of the WGM modulator are discussed elsewhere in detail [18], here we present only the particular parameters related to the integrated WGM EOM used in the OEO.

The modulator has a fibre-to-fibre insertion loss of 5.5 dB. Its optical quality factor Q depends on a chosen mode and varies from 5×10^6 to 9×10^6. The optical spectrum of the cavity is shown in figure 5. The quality factor of the microwave resonator is approximately equal to $Q_M \simeq 70$.

A typical spectrum of the modulated light measured with an optical etalon is shown in figure 6. It should be noted that the amplitude of the carrier cannot be

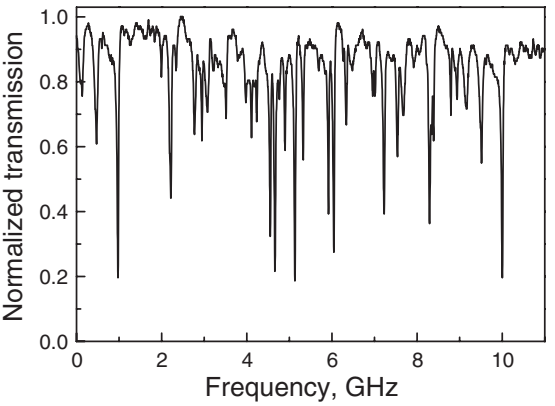

Figure 5. Optical spectrum of the $LiNbO_3$ disc cavity. The coupling efficiency is approximately 80%.

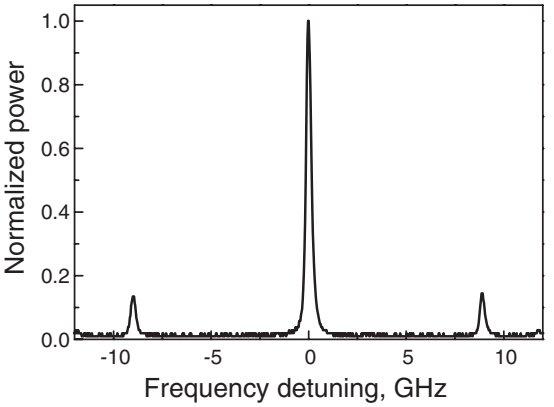

Figure 6. Spectrum of the modulated light after the WGM EOM measured with an optical etalon.

reduced to zero because we do not have critical coupling of the incoming light and the WGM cavity in this particular modulator.

To estimate the efficiency of the modulator for application in the OEO we measured the dependence of the demodulated signal from the photodetector as a function of power of the microwave signal ($E_{M_{\text{in}}}$ in figure 3) sent into the modulator. The result of the measurement is shown in figure 7. Because of the small power of the pump laser radiation (2.5 mW) and nearly complete phase modulation of light, the difference between the input and output microwave power is more than 35 dB. It is worth noting here that for phase modulation and critical coupling the demodulated microwave power is absent. To make our system oscillate either a microwave amplifier must be included in the OEO loop or the optical pump power should be increased.

We obtained self-sustained oscillation in the system with 42 dB microwave amplification. The spectrum of the OEO signal is shown in figure 8. The width of the signal is determined primarily by the pump laser noise. The minimum measured width was about 100 kHz. The scheme should be optimized to reduce

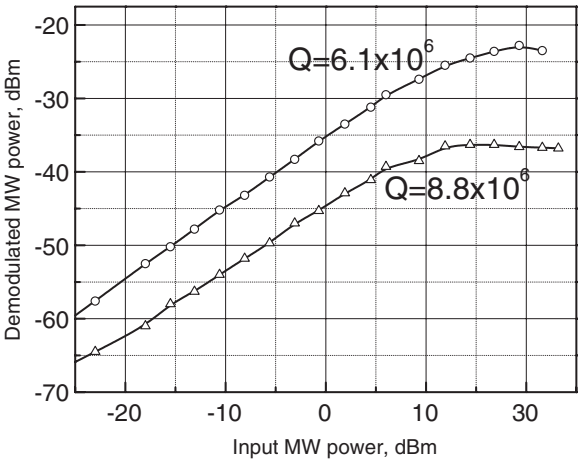

Figure 7. A dependence of the demodulated microwave power, produced after direct absorption of the modulated light on a photodetector, on the input microwave power.

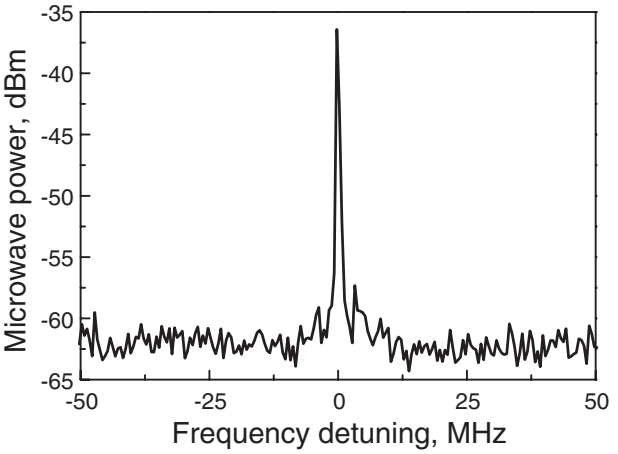

Figure 8. Spectrum of the microwave signal generated in the OEO.

the width and the oscillation threshold, according to the discussion in the theoretical part of the paper.

The optoelectronic oscillator has well pronounced threshold behaviour (figure 9). Power of the generated microwave signal increases approximately linearly with increasing optical power after a certain threshold value of the pump, which is close to the theoretical predictions. Our experimental data, however, are obtained with 42 dB microwave amplification. To obtain characteristics predicted by theory the modulation system should be optimized.

5. Discussion

In comparing the resonant and non-resonant OEOs we should mention that the resonant OEO starts to oscillate and saturates for optical powers approximately

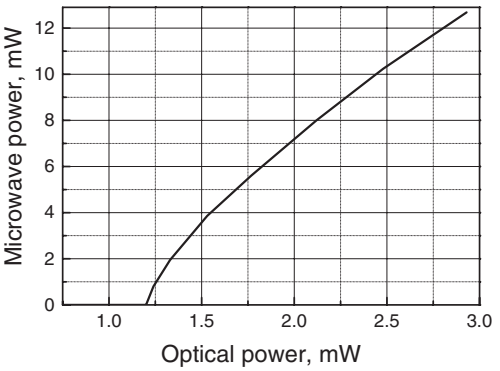

Figure 9. Threshold dependence of the generated microwave signal versus optical pump power.

$(T_M T_c^2)^{-1/2}$ times smaller than the threshold optical power for the non-resonant OEO. While the non-resonant OEO may have better stability, the dynamic ranges of the two devices do not overlap.

The obvious difference between the resonant and non-resonant OEOs is the presence of the cavities for light and for the microwaves. The presence of a cavity increases the strength of the nonlinear interaction. As a result, the non-resonant process saturates for a larger number of microwave photons as compared to the resonant process. The value of the threshold pump power does not depend on the mode volumes for the non-resonant as well as resonant interactions, in a non-intuitive way. However, in the resonant case the threshold value decreases with increasing cavity finesses.

In the resonant OEO the oscillation frequency may appear not at exact coincidence with the optical cavity WGM frequency. Consequently, the transfer of the amplitude fluctuations of the laser into the phase fluctuations of the microwave field occurs. Moreover, the phase diffusion of the pump laser radiation influences the phase diffusion of the microwaves, as well. This effect, however, does not occur in the non-resonant OEO. Therefore, the resonant OEO is suitable for more stable lasers, while the non-resonant OEO is more appropriate for lasers having broader lines.

6. Conclusion

We have studied properties of a resonant optoelectronic microwave oscillator, based on a whispering gallery mode lithium niobate cavity coupled to a microstrip microwave resonator, and compare the properties with those of the non-resonant oscillator. We show that the resonant OEO possesses low oscillation threshold with respect to the optical pump power as well as narrow linewidth of the generated microwave radiation. The size of the resonant OEO may be orders of magnitude less than the size of the non-resonant device. On the other hand, a non-resonant OEO may result in an even narrower linewidth of the generated signal compared with the resonant OEO, which is compensated for by the comparably large optical pump power necessary to achieve oscillations in the non-resonant device. Generally, both resonant and non-resonant OEOs operate in different dynamical ranges and may produce stable microwave signals at frequencies up to 100 GHz

and, therefore, these devices are useful for modern telecommunications and optoelectronics.

Acknowledgments

The research described in this paper was carried out by the Jet Propulsion Laboratory, California Institute of Technology, under a contract with the National Aeronautics and Space Administration and with support from DARPA.

References

[1] Yao, X. S., and Maleki, L., 1996, *J. Opt. Soc. Am.* B, **13,** 1725.
[2] Ji, Y., Yao, X. S., and Maleki, L., 1999, *Electron. Lett.*, **35,** 1554.
[3] Davidson, T., Goldgeier, P., Eisenstein, G., and Orenstein, M., 1999, *Electron. Lett.*, **35,** 1260.
[4] Romisch, S., Kitching, J., Ferre-Pikal, E., Hollberg, L., and Walls, F. L., 2000, *IEEE Trans. Ultrasonics Ferroelectrics Freq. Control*, **47,** 1159.
[5] Yao, X. S., and Maleki, L., 2000, *IEEE J. Quantum Electron.*, **36,** 79.
[6] Poinsot, S., Porte, H., Goedgebuer, J. P., Rhodes, W. T., and Boussert, B., 2002, *Opt. Lett.*, **27,** 1300.
[7] Chang, D. H., Fetterman, H. R., Erlig, H., Zhang, H., Oh, M. C., Zhang, C., and Steier, W. H., 2002, *IEEE Photon. Technol. Lett.*, **14,** 191; 2002, *ibid.*, **14,** 579.
[8] Plourde, J. K., and Ren, C. L., 1981, *IEEE Trans. Michrowave Theory Tech.*, **29,** 754.
[9] Fiedziuszko, S. J., Hunter, I. C., Itoh, T., Kobayashi, Y., Nishikawa, T., Stitzer, S. N., and Wakino, K., 2002, *IEEE Trans. Michrowave Theory Tech.*, **50,** 706.
[10] Yao, X. S., and Maleki, L., 1997, *Opt. Lett.*, **22,** 1867.
[11] Yao, X. S., Davis, L., and Maleki, L., 2000, *J. Lightwave Technol.*, **18,** 73.
[12] Lasri, J., Bilenca, A., Dahan, D., Sidorov, V., Eisenstein, G., Ritter, D., and Yvind, K., 2002, *IEEE Photon. Technol. Lett.*, **14,** 1004.
[13] Qian, S.-X., and Chang, R. K., 1986, *Phys. Rev. Lett.*, **56,** 926.
[14] Lin, H.-B., and Campillo, A. J., 1994, *Phys. Rev. Lett.*, **73,** 2440.
[15] Spillane, S. M., Kippenberg, T. J., and Vahala, K. J., 2002, *Nature*, **415,** 621.
[16] Cohen, D. A., and Levi, A. F. J., 2001, *Solid State Electron.*, **45,** 495.
[17] Cohen, D. A., Hossein-Zadeh, M., and Levi, A. F. J., 2001, *Solid State Electron.*, **45,** 1577.
[18] Ilchenko, V. S., Savchenkov, A. A., Matsko, A. B., and Maleki, L., 2003, *J. Opt. Soc. Am.* B, **20,** 333.
[19] Boyd, R. W., 1992, *Nonlinear Optics* (Boston: Academic Press).
[20] Lu, Y. Q., Xiao, M., and Salamo, G. J., 2001, *Appl. Phys. Lett.*, **78,** 1035.
[21] Abernethy, J. A., Gawith, C. B. E., Eason, R. W., and Smith, P. G. R., 2002, *Appl. Phys. Lett.*, **81,** 2514.
[22] Parsons, N. J., O'Donnell, A. C., and Wong, K. K., 1986, *SPIE Proc.*, **651,** 148.
[23] Brothers, L. R., Lee, D., and Wong, N. C., 1994, *Opt. Lett.*, **19,** 245.
[24] Chen, D. T., Fetterman, H. R., Chen, A. T., Steier, W. H., Dalton, L. R., Wang, W. S., and Shi, Y. Q., 1997, *Appl. Phys. Lett.*, **70,** 3335.